

# A STUDY ON VERTICAL STRUCTURE OF MARINE BOUNDARY LAYER OVER PALAU IN THE TROPICAL WESTERN PACIFIC

<sup>1</sup>G Mahboob Basha,<sup>2</sup>Mohammed Waaiz,<sup>3</sup>U V Murali Krishna,<sup>4</sup>K Krishna Reddy

<sup>1,2</sup>Research Scholar,<sup>3</sup>Research Associate,<sup>4</sup>Professor

<sup>1,2</sup>Department of Physics, Rayalaseema University, Kurnool, Andhra Pradesh, India.

<sup>3</sup>Indian Institute of Tropical Meteorology, Pune, Maharastra, India

<sup>4</sup>Department of Physics, Yogi Vemana University, Kadapa, Andhra Pradesh, India

**Abstract**— We are carrying out research at Palau Islands focusing on the Pacific Area Long-term Atmospheric observation for Understanding of climate change (PALAU) project to understand the mechanism of cloud-precipitation processes, land-atmosphere and air-sea interactions over the warm water pool, focusing on seasonal and intra-seasonal variations. We installed several ground based remote sensors at Peleliu and Aimeliik experimental sites in the Palau. For the present study, Wind Profiler Radar (WPR) and Disdrometer are utilized for preliminary understanding of the marine boundary layer (MBL) evolution, diurnal and seasonal variation of precipitating cloud systems associated with easterly and westerly monsoon. In the present study, long-term (or four year) observations of the marine boundary layer height using wind profiler radar are utilized to estimate ventilation coefficient, a critical parameter in determining air pollution concentration near the surface which signifies the ability for natural ventilation of air over Palau in Tropical Western Pacific Ocean during the period from April 2003 to March 2007. In addition, MBL observations revealed that well-distinguishable features during westerly, easterly and transition period.

**Index Terms**—Marine Boundary Layer, Wind Profiler Radar, Monsoon, Radar Reflectivity, Ventilation Coefficient

## I. INTRODUCTION

Due to lack of direct measurements of boundary layer height and of suitable measurements that could be used to estimate it[1], the boundary layer height is less common in the climatological literature. This problem may be partially remedied through analysis of new data sources like observations by radio occultation measurements from global navigational satellite systems[2][3]<sup>2,3</sup>, aerosol observations from satellites[4], Lidar[5] and Sodar[6]. Other types of observations, including Wind-profiling and boundary layer Radar and Ceilometer[7-9] have been used to estimate boundary layer height. During the past one decade Doppler wind radar profilers (WPR) that operate near 1 GHz have been use in boundary layer dynamics and precipitation research. The advantage of this WPR is to measure directly the vertical wind component within a convective environment. The WPR have been used extensively in numerous field campaigns during the past one decade [10]. WPR observations yield time height cross sections of equivalent reflectivity, Doppler velocity and spectral width that illustrate the evolution of boundary layer and precipitating clouds systems.

## II. LOCATION, DATA AND MEASUREMENT TECHNIQUES

Institute of Observational Research for Global Change has conducted the observational project PALAU (Pacific Area Long-term Atmospheric observation for the Understanding of climate change) over Peleliu Island (7.05°N, 134.27 °E) and Aimeliik state of Babeldaob Island (7.45° N, 134.47° E) of Republic of Palau is shown in Fig.1. National Weather Service (NWS) which is confided by National Oceanic and Atmospheric Administration (NOAA) is located at Koror (7.33°N, 134.48°E) the capital of Palau. At Aimeliik Observatory, Wind profiler radar (WPR) with Radio acoustic sounding system, Impact type disdrometer, Micro Rain Radar, Ceilometer, Microwave Radiometer and Automatic Weather Station (AWS), Ceilometer are installed and continuous gathering data.

Aimeliik is located in the high island of Babeldaob [in the Palau (508 Sq. km) archipelago], which is one of the largest islands in the western Pacific Ocean. Babeldaob Island is partly elevated limestone and partly volcanic. The vegetation in this island varies from the mangrove swamps of the coast, with trees often from 10–16 meters high; to the savannah type grasslands of the near interior which support palms and pandanus, and the densely forested valleys further inland. WPR is in continuous operation since 08 March 2003. For the present study one year data from 15 March 2003 to 14 March 2004 has been utilized. Observations with the Aimeliik WPR were carried out continuously since 09 March 2003[11]. Although Fig. 2(a) shows the observation period as of the end of September 2004, wind profiler operation is continued till date. The wind profiler routinely provides hourly averaged vertical profiles of horizontal wind velocity from 0.1 to 4.0 km above ground with 60 m vertical resolution in clear-air and also 200 m vertical resolution in cloudy and precipitating conditions.

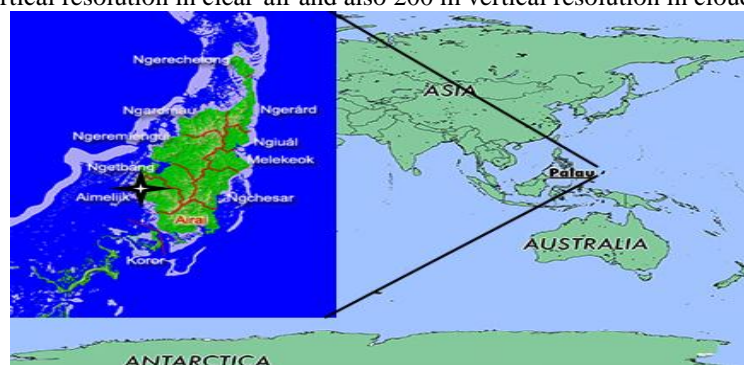


Figure 1: Map showing location of Aimeliik Observatory over Palau Islands, in Pacific Ocean

A radio acoustic sounding system (RASS) provided vertical profiles of virtual temperature, which we later transformed into profiles of virtual potential temperature [12]. The upper range of these profiles typically reaches 500–1000 m above ground. During the observational period, no availability of the data for several days was mainly due to external power failure, system maintenance, and severe weather hazards. For detailed WPR description, data collection and operation strategy [13]. Upper air sounding is carried out by Koror National Weather Service (NWS) which is located about 10 km south of Aimeliik observatory. Balloons are launched twice a day i.e. around 0000 and 1200 UTC. Additional 2 or 3 balloons released by the NWS during intensive observational periods.

The availability of measured data depends strongly on wind profiler system reliability and is an important criterion for wind climatology, numerical weather prediction and operational applications. The height coverage of WPR depends both on system characteristics and meteorological conditions (especially on humidity and hydrometeor). For the maximum range is determined by the strength of the backscattered power in proportion to noise. Therefore, the actual height coverage of data measured by the WPR is more or less variable. Figure 2(b) shows the relative availability of wind intensive observational periods. The WPR is very sensitive to precipitation particles, so that the height coverage is greatly increased up to 6 km in the high mode (with 80% probability).

*Intercomparison of WPR and Radiosonde Wind Measurements*

To evaluate the performance of the Wind profiler radar (WPR), we have performed a statistical intercomparison (non-precipitating days) with the simultaneous observation of radiosonde at Koror (0000 and 1200 UTC) shown in Fig 2(c). The two locations are about 10 km apart and presuming that the spatial homogeneous between the two measurements. Comparison is made only when valid data are available from radiosonde and wind profiler. To avoid the several scatter plots of intercomparison, only a typical scatter plot around 2.9 km for wind speed is shown in Fig. 2(d). The correlation coefficient is around 0.92, which is probably acceptable in view of the differences in measurement technique. Figure 2(e) and 2(f) shows the results are encouraging and evident from the wind speed and wind direction deviations.

**III RESULTS AND DISCUSSION**

*Evolution of MBL Height*

For the present study, we analyzed four year variations in the Marine Boundary Layer (MBL) height over Palau using wind profiler radar and Radiosonde data. Wind profiler radar offers the unique ability to directly measure vertical motion profiles through precipitating and non-precipitating cloud systems (Reddy et al. 2002). So wind profiler radars can be used to determine the MBL height during both precipitating and non-precipitating events. As an example, time height profile of radar reflectivity during 02<sup>nd</sup> July 2003 (non-precipitating event) is shown in Fig. 3. The solid line in Fig. 3 represents the hourly averaged MBL height derived from radar reflectivity during 0800 to 1800 local time (LT) on the same day. When the amount of incoming solar radiation increases in the morning hours, then MBL height also increases and reaches its maximum in the afternoon. When the solar elevation decreases, the available energy is small, so the thermally-driven turbulence decays and vertical mixing decreases and hence the MBL height decreases.

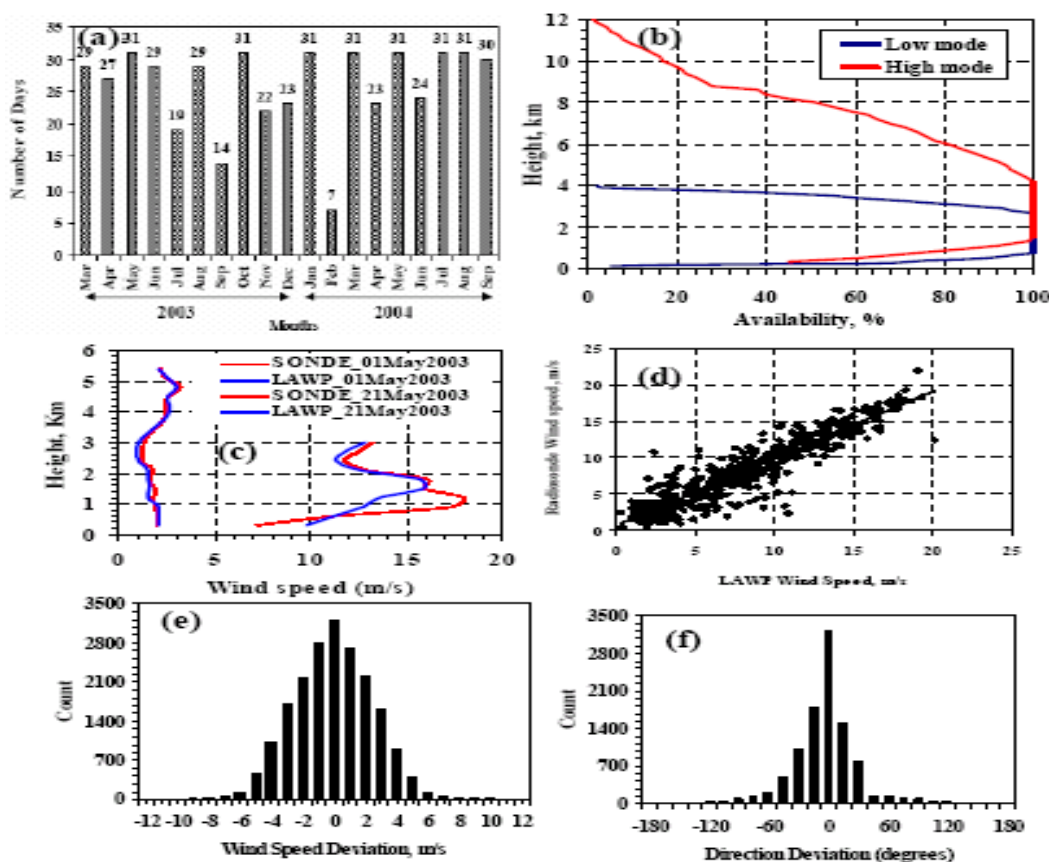


Figure.2 (a) Wind profiler radar data collection period, (b) WPR data availability during high and low mode operation, (c) comparison of WPR and Radiosonde wind measurement, (d) Scatter diagram between WPR and Radiosonde winds at 2.9 km during May 2003 to 31 Sept. 2003, (e) WPR-Wind Speed deviation and (f) WPR-Wind direction deviation

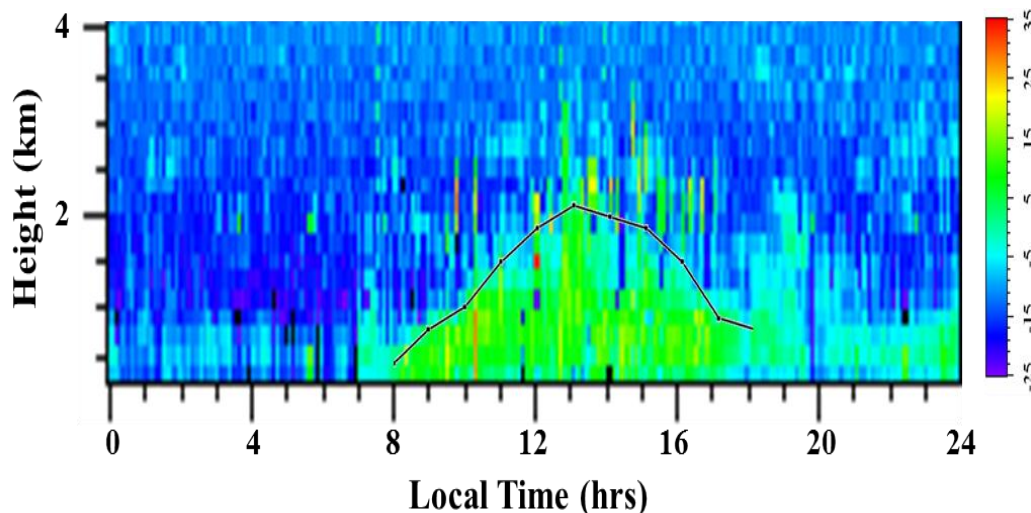


Figure 3: Time height profile of radar reflectivity during 02<sup>nd</sup> July 2003 over Palau. The solid line represents the hourly averaged MBL height derived from radar reflectivity.

#### Comparison of MBL height derived from WPR and Radiosonde Measurements:

Maximum mixing depth (MMD) derived from individual radiosonde profile are compared with the mean MBL height derived from WPR measurement. 30 minutes average of MBL height measured between 0000& 0030 GMT and 1200& 1230 GMT using WPR during non-rainy days are compared with the radiosonde profile during respective days. The scatter plot of the boundary layer depths derived from the wind profiler and radiosonde shown in Fig. 4. It shows a reasonably good agreement between the two methods. The observed discrepancies are expected because; radiosonde provides a “snapshot” of the state of the atmosphere as they ascend. Therefore, the mixing height determined from radiosonde data represents a point measurement in space and time. Hence, WPR can be used to monitor the boundary layer height in a continuous fashion as radiosonde data is not available continuously.

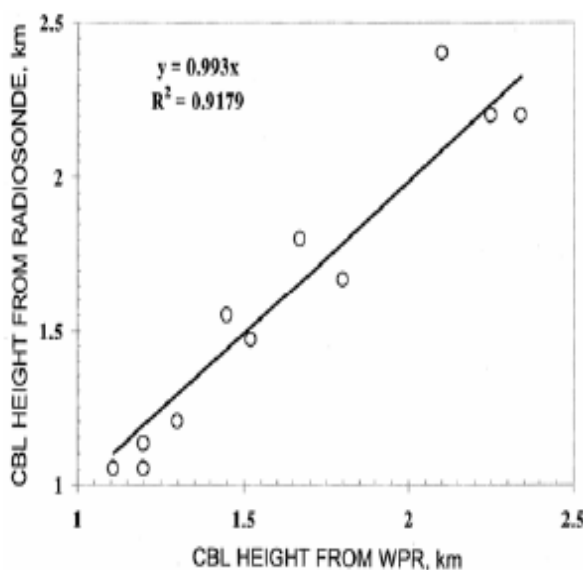


Figure.4 : Scatter plot of convective boundary layer heights estimated from the wind profiler and radiosonde observations

#### Temporal Variation of MBL height and VC

Diurnal evolution of mean MBL height during 0800 to 1800 LT is shown in Fig 5a. It is observed that the MBL depth is low during morning hours, increases gradually with time after sunrise and reaches a higher value at noon hours and starts decreasing in the evening. This is the general behaviour of day time boundary layer during clear air days. The increased MBL height after sunrise may be connected to the start of the sea breeze from the surrounding marine atmosphere and hence turbulence becomes stronger and the MBL height grows steadily after sun rise. The evolution of the daytime boundary layer can influence the aerosol particle concentration and size distribution at the ground level. In the early morning hours when the MBL depth is low, there can be accumulation of pollutants near the surface. After sunrise, the boundary layer starts evolving with time. Hence the pollutants trapped in the ground based stable layers during the previous night are dispersed and transported to other regions of the lower atmosphere by turbulent mixing. During evening hours, the pollutants emitted can be constrained at the lower heights in the boundary layer and can remain until early morning hours due to the formation of nocturnal stable boundary layer. Thus the diurnal behaviour of the boundary layer plays an important role in aerosol particle concentration at the ground level. This is further evident from the variation of Ventilation Coefficient (VC).

Figure 5b and 5c represents the temporal variation of average wind speed within the boundary layer and ventilation coefficient respectively. The diurnal variation of VC shows low values during early morning hours, it gradually increases and reaches maximum value during the noon hours and decreases in the evening. This indicates the high dispersive capacity of MBL during afternoon hours.

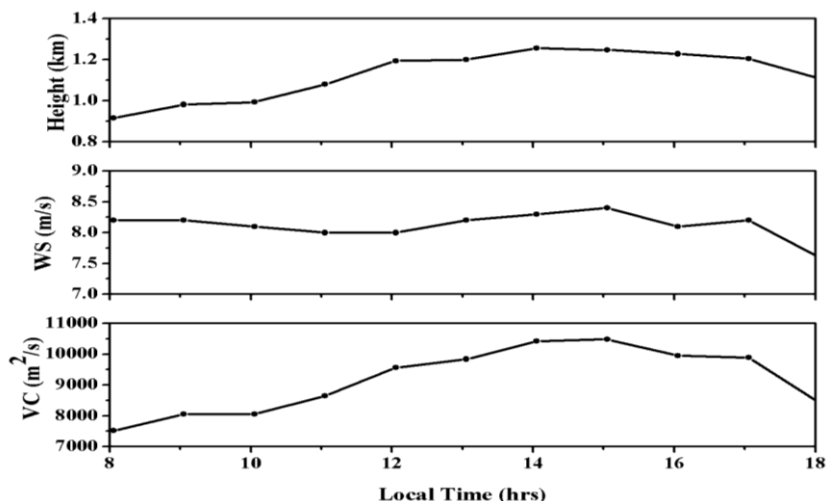


Figure 5: Diurnal evolution of (a) MBL height (b) mean wind speed and (c) ventilation coefficient within MBL during 0600 to 1800 local time on 15<sup>th</sup> January, 2004.

Monthly and Seasonal Variations of VC

Figure 6 show the monthly averaged diurnal variation of MBL height during 2003 to 2007. The months of February, April and November show the longest and highest MBL heights whereas the months June, August and September the lowest MBL height. The higher MBL height during April and November is due to higher sunshine hours. However the higher MBL height during February is due to availability of less number of data during February. For this reason, we will not consider the MBL height in February as maximum in the calculation of ventilation coefficient. MBL heights are lowest during June, August and September which corresponds to the lowest average sunshine hours.

To study the monthly variation of Ventilation Coefficient (VC), monthly mean of maximum MBL height for each day and the corresponding wind speed within the boundary layer are given in Fig. 7(a) and (b) for the year 2004. This is used to estimate the monthly average of VC (Fig. 7(c)). It is apparent that VC has the highest value during August (~ 8122 m<sup>2</sup>s<sup>-1</sup>) and lowest during January (5424 m<sup>2</sup>s<sup>-1</sup>). The MBL height is high during April and this reaches an average value of ~ 1.45 km, whereas lower values are observed in September (~ 1.3 km). During the other months the MBL height varies in the range ~ 1.3 to 1.5 km. Maximum wind speed is observed during June, July and August. It can be seen that the variation of VC during the period November to April is influenced both by the MBL height and wind speed within the MBL, whereas during May to October, it closely follows the same type of variation as that of the wind speed. Note that the MBL height does not vary much from July to November. It can be noted from Fig. 7 that the annual variation of MBL height is not as drastic as that of wind speed, and it is the larger increase in wind speed rather than MBL height that results in high VC during the monsoon months.

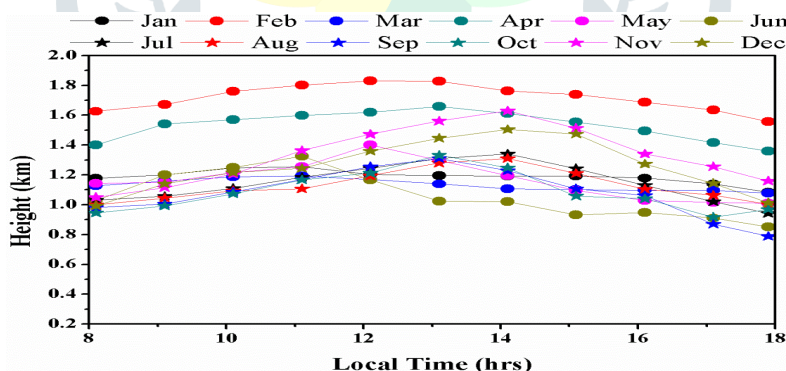


Figure 6: Monthly mean of daily hourly averaged MBL heights over Palau.

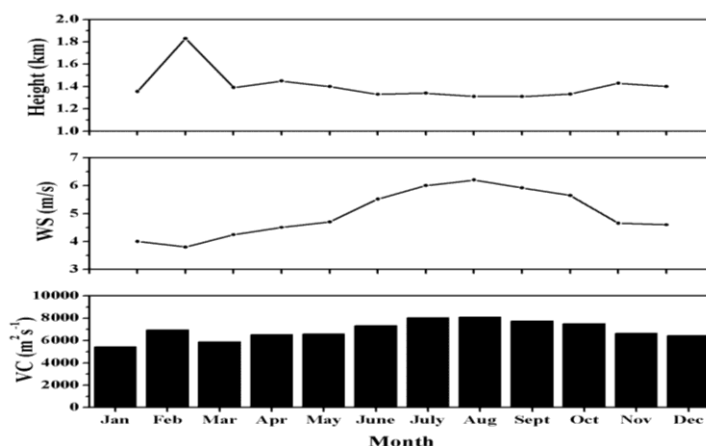


Figure 7: Monthly variation of mean noon-time (a) MBL height (b) Wind Speed and (c) VC over Palau during April, 2003 to March, 2007.

To study the Seasonal variation of VC, the data is divided into four groups (Table 1) corresponding to Easterly (late December to April), Easterly to Westerly transition (May and June), Westerly (July to October) and Westerly to Easterly transition (November and Early December) periods. The average values of VC and mean noon time MBL height during April 2003 to March 2007 is shown in Table.1. It is observed that VC is high during Westerly monsoon period ( $7020 \text{ m}^2\text{sec}^{-1}$ ) and low during Easterly to Westerly transition period ( $5120 \text{ m}^2\text{sec}^{-1}$ ). During Easterly monsoon period VC is  $5670 \text{ m}^2\text{sec}^{-1}$ , whereas during Westerly to

Easterly transition VC is found to be  $6230 \text{ m}^2\text{sec}^{-1}$ . The high value of VC during Westerly monsoon period is due to high wind speed. Along with the high value of VC, wash out processes by precipitation can result in a cleaner environment. However, low values in wind speed results in low values of VC during Westerly to Easterly transition period. This may be attributed to the increase of anthropogenic aerosol loading during Westerly to Easterly transition period which has profound effects on the climate change over this region (Intergovernmental Panel on Climate Change (IPCC) report, 2001). The estimated VC for Tehran region (Iran) and found that the VC values for spring and summer were higher than those for fall and winter[14]. At Fort Simpson, Northwest Territories region found winter VC extremely low on most days due to low mixing depths frequently coupled with light winds through mixing layer. However in the present study, we reported low values in VC during transition period, moderate VC during Easterly and high VC during Westerly monsoon period.

**Table.1:** Seasonal variation of MBL height and VC over Palau during April 2003 to March 2007.

Season/Climate	Months	Mean noon time MBL height (km)	Ventilation Coefficient ( $\text{m}^2\text{s}^{-1}$ )
Easterly monsoon	Late December to April	$1.28 \pm 0.26$	5670
Easterly to Westerly monsoon Transition	May and June	$1.11 \pm 0.17$	5120
Westerly monsoon	July to October	$1.19 \pm 0.21$	7020
Westerly to Easterly monsoon Transition	November to Early December	$0.97 \pm 0.16$	6230

#### Marine Boundary Layer evolution during different seasons

Figure 8 shows the time-height cross-section reflectivity observed on typical days during different seasons using WPR. During relative dry days the strong reflectivity is observed during morning hours corresponds to the morning transition or the morning rise of the inversion. The significant echo region appears in the lowest observational heights and ascends gradually, reaching a maximum height in the afternoon hours. This strong echo region marks the height of the daytime marine boundary layer (MBL). These features can be used for understanding the triggering of cumulus convection.

Time series of the daily maximum MBL height, as a function of Julian day of the year, are presented in Fig. 9, showing both individual daily values and a smoothed 5-day running mean. The smoothed MBL height is at or near its maximum in the month of April, before the onset of westerly monsoon period and then decreases with time until July, increases slightly and then decreases again reaching its minimum values during the month of September. The MBL height partially recovers to a second but lower set of peaks at the end of westerly monsoon period, then increases again.

Figure 10(a) shows the evolution of MBL during easterly monsoon period. On these days, MBL developed at morning 0600 hrs and afterwards, the MBL grows steadily and reaching its peak at about 1400-1500 hrs and coming down thereafter. The deepening of the MBL is observed in the late afternoon during easterly monsoon period. Figure 10(b) shows the evolution of MBL in westerly monsoon period. On these days, a different scenario has been observed. A shallow MBL confined to about 1.1 km is observed on both the days. This is because during the westerly monsoon, boundary layer will be rich in moisture. So, most of the radiation will be utilized for the evaporation process, which results in a shallow MBL. One more cause for the shallow MBLs during the westerly monsoon days may be due to the increased upper level clouds that can reduce the incoming solar radiation. Similar features have been observed on most of the days in each category during the observational period.

To explain the shallow MBL heights during the westerly monsoon period, we investigated the effect of surface solar radiation and low level cold air advection on MBL height. Surface solar radiation plays an important role in driving the MBL, and variations due to clouds or aerosols can have a pronounced effect on MBL height. Figure 11 shows the correlation between MBL height and surface solar radiation. Positive correlation exists between MBL height and surface solar radiation indicating that the MBL height increases with solar radiation.

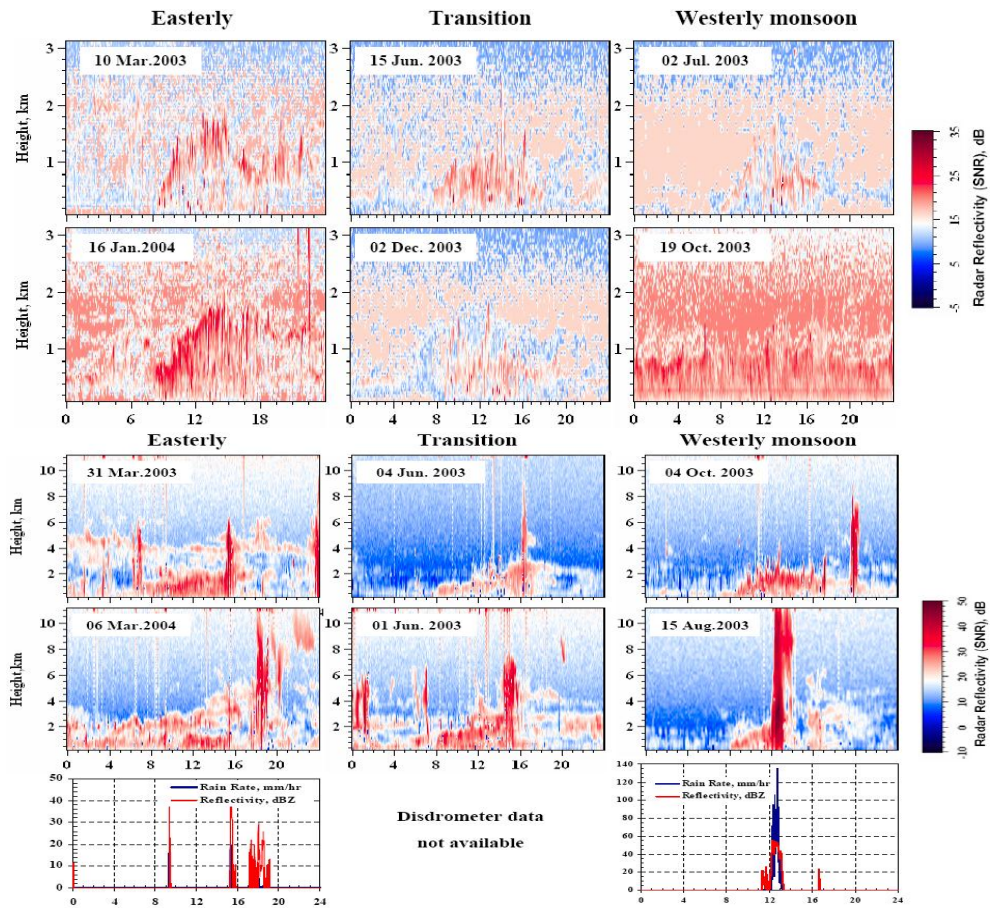


Figure 8: Time-height cross section of the Aimeliik wind profiler (vertical beam) range-corrected reflectivity (SNR) during (a) ‘dry’ and (b) ‘wet’ convection days during different seasons. (a) ‘dry’

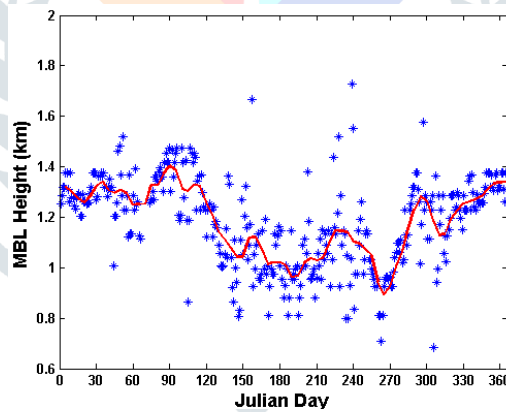


Figure 9: Time series of maximum daily boundary-layer depths (km) as a function of the Julian day of the year (blue stars). The red line is the smoothed interpolation of the data.

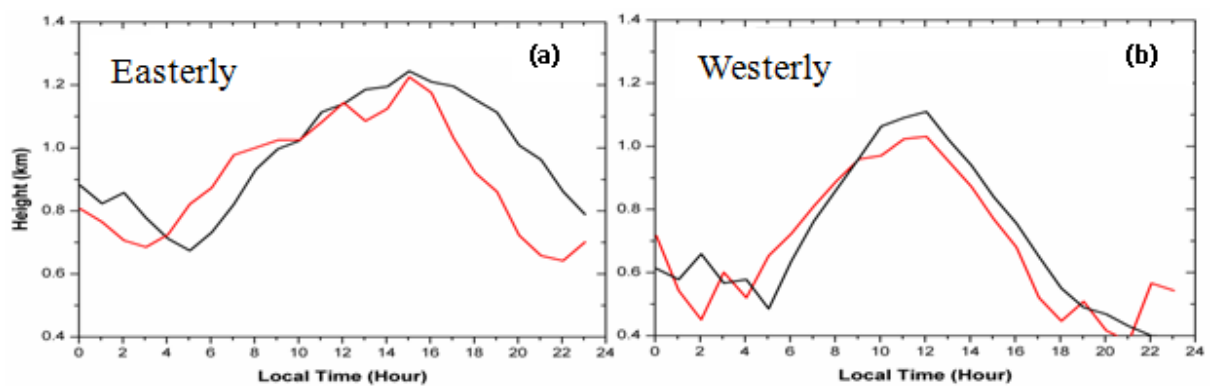


Figure 10: Evolution of MBL on two (a)Easterly monsoon (b) Westerly monsoon days.

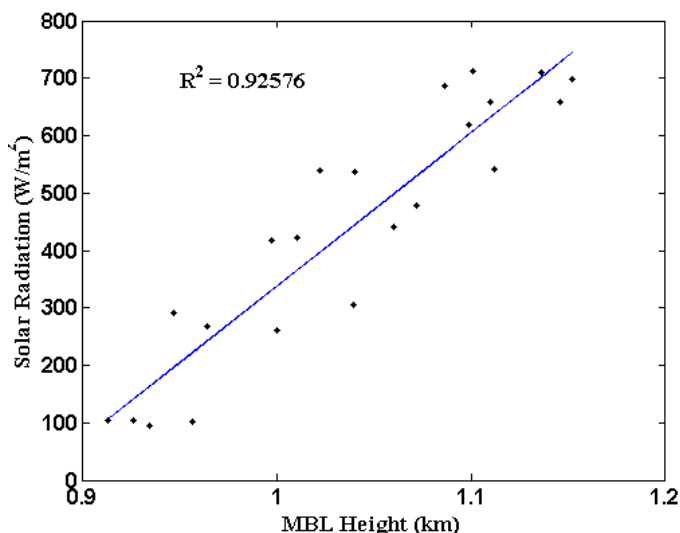


Figure 11: Correlation between MBL height and surface solar radiation.

Table 2 contains monthly means of solar radiation ( $\text{W m}^{-2}$ ) and the daily maxima solar radiation ( $\text{W m}^{-2}$ ). Overall, the large values of both solar radiation measures for the easterly monsoon period are indicative of mostly cloud-free conditions. The daily maximum MBL heights occur in April with values of approximately between 1.2 to 1.5 km, decreasing to 0.9 to 1.1 km in July. Due to large solar radiation during April, maximum MBL heights are observed.

**Table.2:** Monthly mean solar radiation (top number); and monthly mean hourly maximum solar radiation, *SR* (bottom number).

Month	Jan	Feb	Mar	Apr	May	Jun	Jul	Aug	Sep	Oct	Nov	Dec
Mean	194.9	206.3	212.3	232.2	178	198.3	186.9	213.4	214	210.1	198.9	189.5
Max	832.9	814.7	804.3	860.2	684.6	745.7	743	797.2	814.1	845.4	796.6	710.5

Cold-air advection within the boundary layer can help reduce MBL heights by counter-acting the warming due to surface heating from solar radiation. Figure 12 shows temperature advection for both the easterly and westerly monsoon periods. The advection is calculated as the temperature difference between monsoon period and the average temperature for the whole observational period, multiplied by the westerly wind component. Increased cold-air advection during the westerly monsoon period is evident, especially at lower levels and afternoon to evening hours. The strongest cold-air advection for these months begins in the early afternoon hours, after which the MBL decreases its height gradually. This cold-air advection is associated with the push of marine air into the inland region that occurs with the afternoon sea-breeze circulation. Low-level cold-air advection will increase the stratification and will counteract the warming due to solar insolation, and will contribute to the shallower MBL heights during westerly monsoon period.

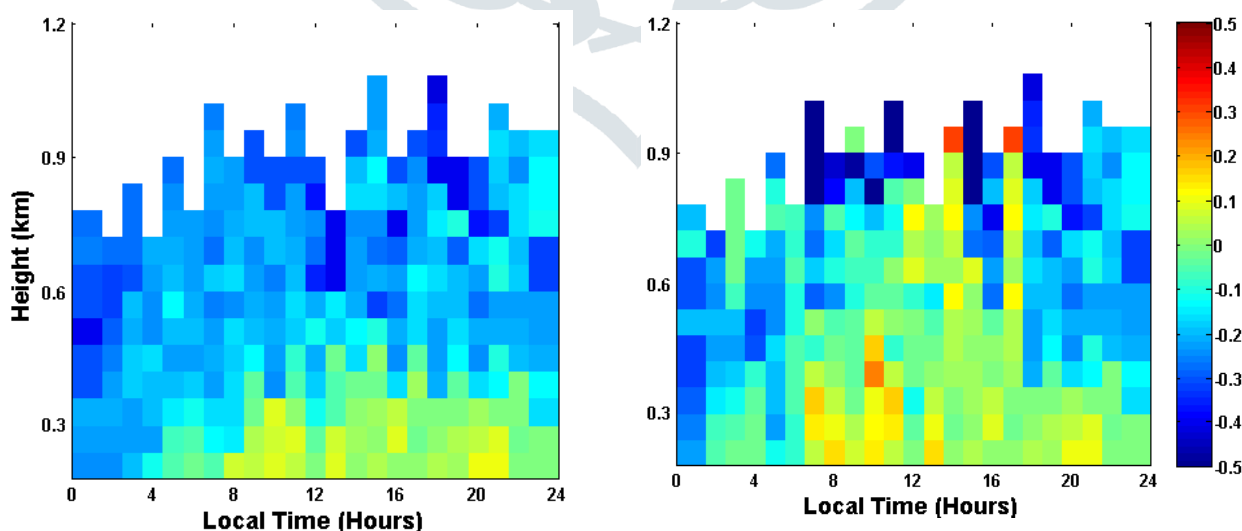


Figure 12: Diurnal mean time–height cross section of virtual temperature advection for (a) Easterly (b) Westerly monsoon period.

#### IV. SUMMARY AND CONCLUSION

The Wind profiler radar (WPR) is continuously operated since 09 March 2003. To check the WPR performance, a comparison study with Korrer radiosonde data is carried out. The results show fairly good agreement between the two measurements considering the spatial separation and data acquisition. The MBL height shows a diurnal variation with its maximum in the afternoon and decreases slowly reaching its minimum in the night. The seasonal variability of MBL height shows a maximum in the month of April and minimum in the month of

September. The effect of surface solar radiation and low level cold air advection on MBL height is investigated. It is clear that, surface solar radiation is responsible for the maximum MBL height in the easterly monsoon period and cold air advection from the surrounding marine atmosphere is responsible for the shallow MBL heights during the westerly monsoon period.

#### REFERENCES

- [1] Liu, S., and X.-Z. Liang (2010) Observed diurnal cycle climatology of planetary boundary layer height, *J. Clim.(USA)*, 23, 5790–5809.
- [2] Guo, P., Y.-H. Kuo, S. V. Sokolovskiy, and D. H. Lenschow (2011) Estimating atmospheric boundary layer depth using COSMIC radio occultation data, *J. Atmos. Sci.(USA)*, 68, 1703–1713.
- [3] Ao, C. O., D. E. Waliser, S. K. Chan, J.-L. Li, B. Tian, F. Xie, and A. J. Mannucci, (2012) Planetary boundary layer heights from GPS radio occultation refractivity and humidity profiles, *J. Geophys. Res.(USA)*, 117, D16117, doi:10.1029/2012JD017598.
- [4] McGrath-Spangler, E. L., and S. Denning (2012) Estimates of North American summertime planetary boundary layer depths derived from space-borne lidar, *J. Geophys. Res.(USA)*, doi:10.1029/2012JD017615.
- [5] Tucker, S. C., C. J. Senff, A. M. Weickmann, W. A. Brewer, R. M. Banta, S. P. Sandberg, D. C. Law, and R. M. Hardesty (2009) Doppler lidar estimation of mixing height using turbulence, shear, and aerosol profiles, *J. Atmos. Oceanic Technol.(USA)*, 26, 673–688.
- [6] Lokoshchenko, M. A. (2002) Long-term sodar observations in Moscow and a new approach to potential mixing determination by radiosonde data, *J. Atmos. Oceanic Technol.(USA)*, 19, 1151–1162.
- [7] Angevine, W. M., A. B. White, and S. K. Avery, (1994) Boundary layer depth and entrainment zone characterization with a boundary-layer profiler. *Boundary Layer Meteorology (NETHERLANDS)*, 68, 375–385.
- [8] Bianco, L., and J. M. Wilczak, (2002) Convective boundary layer depth: improved measurement by doppler radar wind profiler using fuzzy logic methods. *J. Atmos. Oceanic Tech(USA)*, 19, 1745-1758.
- [9] van der Kamp, D., and I. McKendry (2010) Diurnal and seasonal trends in convective mixed layer heights estimated from two years of continuous ceilometer observations in Vancouver BC, *Boundary Layer Meteorol.(NETHERLANDS)*, 137, 459–475.
- [10] K.S.Gage, C.R.Williams, W.L.Clark, P.E. Johnston, and D.A.Carter, *J. Atmos.Ocean. Tech.(USA)*, 19, 843 (2002).
- [11] Williams, C.R., W.L.Ecklund, and K.S.Gage, *J. Atmos.Ocean. Tech. (USA)*, 12, 996 (1995).
- [12] K.K.Reddy, T. Kozu, Y.Ohno, K. Nakamura, A.Higuchi, K.Madhu Chandra Reddy, P.Srinivasulu, V.K.Anandan, A.R.Jain, P.B.Rao, R.RangaRao, G.Viswanthan, and D.N.Rao, *Radio Sci. (USA)*, 37, 14-1 (2002).
- [13] K.K.Reddy, B. Geng, H.Yamada, H.Uyeda, R.Shirooka, T.Ushiyama, S.Iwasaki, H.Kubota, T.Chuda, K.Takeuchi, T.Kozu, Y.Ohno, K. Nakamura, D.N.Rao, Monsoon precipitation characteristics over Asia and Western Tropical Pacific Ocean, 6th International GAME Conference, Kyoto International Community House, Kyoto, Japan, 3-5 December 2004.
- [14] Ashrafi, K., Shafie-Pour, M., & Kamalan, H. Estimating temporal and seasonal variation of ventilation coefficients. *International Journal of Environmental Research*, 3, 637–644 (2009).

